Transient infiltration from ephemeral streams: A field experiment at the reach scale

Jordi Batlle-Aguilar[1] and Peter G. Cook[1,2]

Received 17 February 2012; revised 13 September 2012; accepted 26 September 2012; published 14 November 2012.

[1] An infiltration experiment at the stream reach scale was performed to estimate infiltration rates beneath an ephemeral, losing stream during streamflow events. At a time when the stream was dry, a 7 m stream section was dammed upstream and downstream using metal sheets. During a 5 day period water was pumped into the isolated section of the stream, and the surface water level was maintained at three successive increasing stages. The infiltration rate at each water level was thereby equal to the pumping rate required to maintain that water level. The advantages of the method are that it samples a much greater area than traditional methods and provides information on infiltration through stream banks as well as through the streambed. Experimental results provide insight into transient infiltration and recharge processes beneath ephemeral streams. Although the experiment continued for 5 days, infiltration during the first hour accounted for 19% of the total infiltration. High transient infiltration rates were also observed following each increase in stream stage. Experimental infiltration rates were used to calibrate a two-dimensional model developed within Hydrus, which was subsequently used to estimate infiltration associated with a natural flow event in the same stream reach. During the natural flow event, the total infiltration was 33% greater than would have been estimated assuming steady state infiltration rates. Dry antecedent moisture content controls the transient infiltration rate and hence increases the total infiltrated volume during flow events, but it does not increase the aquifer recharge.

Citation: Batlle-Aguilar, J., and P. G. Cook (2012), Transient infiltration from ephemeral streams: A field experiment at the reach scale, *Water Resour. Res.*, *48*, W11518, doi:10.1029/2012WR012009.

1. Introduction

[2] In many arid and semiarid areas, groundwater recharge mainly occurs through water infiltration from intermittent or ephemeral streams [*de Vries and Simmers*, 2002; *Dunkerley*, 2008]. The streambed saturated hydraulic conductivity is the main hydrogeologic parameter controlling groundwater recharge, but is characterized by a high spatial variability [*Bruen and Osman*, 2004; *Calver*, 2001; *Kalbus et al.*, 2009]. An important limitation of methods traditionally used to estimate infiltration rates and streambed hydraulic properties is their limited spatial resolution, and so they are usually not considered sufficiently reliable for quantifying infiltration at the catchment scale [*Berndtsson and Larson*, 1987]. Nevertheless, point testing methods such as seepage meters [*Lee*, 1977; *Murdoch and Kelly*, 2003], disc permeameters [*Perroux and White*, 1988] and ring infiltrometers [*Dunkerley*, 2008; *Guyonnet et al.*, 2000] are widely used.

[3] Quantifying direct infiltration from ephemeral streams needs to deal with changes in infiltration rates over time. *Horton* [1940] showed that ponded infiltration in soils decreases with time until a constant rate is reached. Laboratory infiltration experiments [*Childs and Bybordi*, 1969; *Mein and Larson*, 1973] confirmed that water infiltration is characterized by a transient period of high infiltration rates at the beginning of ponding, followed by a subsequent nearly steady state period. Later, *Blasch et al.* [2006] showed the importance of these processes to ephemeral streams. It is also likely that a transient infiltration period might occur after any change of the stream water level, although we are not aware of any studies that have examined this phenomenon. Measuring steady state infiltration rates is relatively easy, but unfortunately natural processes are far from steady state, and surface water levels in streams and rivers continuously fluctuate. Ephemeral streams in semiarid areas are characterized by irregular and intermittent flow events highly dependent on storm episodes.

[4] Previous studies that have directly estimated groundwater infiltration and/or aquifer recharge from streams have focused mostly on the use of seepage meters [*Fritz et al.*, 2009; *Rosenberry and Pitlick*, 2009; *Rosenberry et al.*, 2012]. A variety of different indirect methods to calculate

[1]National Centre for Groundwater Research and Training, School of the Environment, Flinders University, Adelaide, South Australia, Australia.
[2]Water for a Healthy Country National Research Flagship, Division of Land and Water, Commonwealth Scientific and Industrial Research Organization, Adelaide, South Australia, Australia.

Corresponding author: J. Batlle-Aguilar, National Centre for Groundwater Research and Training, School of the Environment, Flinders University, GPO Box 2100, Adelaide, SA 5001, Australia. (jordi.batlleaguilar@flinders.edu.au)

©2012. American Geophysical Union. All Rights Reserved.
0043-1397/12/2012WR012009

infiltration fluxes based on measurements of changes in soil water content [*Dahan et al.*, 2008; *Sophocleous*, 1991; *Sorman et al.*, 1997], soil temperature [*Constantz et al.*, 2002; *Ronan et al.*, 1998] or water table mounding [*Dagès et al.*, 2008] have also been used. However, although water infiltration from streams occurs vertically and laterally due to the influence of gravitational and matric potential forces, respectively, one-dimensional models are mostly used for interpreting field monitoring data [*Blasch et al.*, 2006]. While these models are probably reasonable in wide streams with flat streambeds [*Ronan et al.*, 1998], *Constantz et al.* [2002] showed that neglecting lateral infiltration in narrow and relatively channelized streams could lead to underestimation of water infiltration by up to 70%.

[5] In this study we provide a combination of reach-scale field experimentation and two-dimensional numerical modeling to estimate the transient and steady state behavior of water infiltration in ephemeral streams. While most of the above methods rely on inferring infiltration from changes in measured parameters such as soil moisture or temperature, our experiment is analogous to a large-scale infiltration experiment. We artificially flooded a stream reach for a period of 5 days, and measured the volume of water that was pumped into the stream to maintain a constant water level, thus providing a direct measure of the infiltration rate. The experiment was carried out at increasing surface water levels to investigate the relationship between infiltration rate and stream stage. The advantages of the method are that it samples a much greater area than traditional methods without disturbing the streambed, and that it provides information on infiltration through stream banks as well as through the streambed.

[6] Directly measured infiltration rates were subsequently modeled, and the resulting calibrated model was used to evaluate the relative contribution of transient and steady state infiltration under natural flow events. We highlight the relative importance of transient infiltration at the beginning of flow events and show that the transient period can last for several days and hence that the use of steady state infiltration rates can substantially underpredict total stream infiltration. We also provide an analysis of stream water infiltration and aquifer recharge, terms commonly used as synonymous despite their significantly different connotation. In particular, we estimate the minimum duration of a flow event required to generate recharge as a function of the soil moisture conditions and water table depth.

2. Study Site

[7] The experimental site is located close to McLaren Vale, 30 km south of the city of Adelaide, South Australia (Figure 1). Pedler Creek is the largest (107 km^2) of the subbasins forming the Willunga Basin (317 km^2), and has a total creek length of 180 km. Pedler Creek only flows for 31–130 days per year (average of 83 d yr^{-1} for the period 2000–2011), with most flow events occurring between July and September. The mean annual flow volume is approximately 1.8×10^6 m^3 (period 2000–2011; gauge ID 5030543), and daily discharges are rarely higher than 4×10^5 m^3 d^{-1}. Pedler Creek and its tributaries provide a potential source of direct recharge to the underlying aquifers. Mean annual rainfall in the basin is approximately 515 mm, with 65% of the precipitation concentrated between winter and early spring months (June to September). Daily maximum temperatures, ranging between 35 and 43°C, are registered in January and February, while daily minimum temperatures, rarely below 5°C, are registered between July and August.

[8] Hydrogeologically, the basin is a multilayered aquifer system, the Quaternary unconfined aquifer overlying confined sand and limestone aquifers. Quaternary sediments are

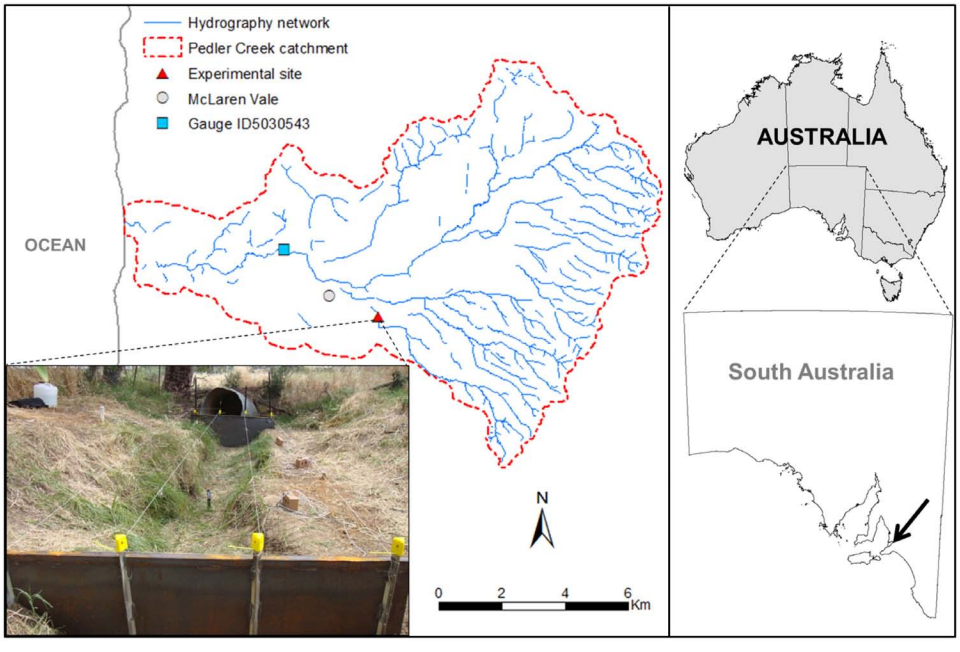

Figure 1. Location of the experimental site. The inset shows the 7 m long creek section isolated using metal sheets.

characterized by poorly sorted clayey sand, sand and sandy clay, with grain size from fine to coarse. The water table depth is mostly less than 10 m. Groundwater is primarily used for vineyard irrigation, and its quality is generally good (electrical conductivity mostly ranging between 670 and 2500 μS cm^{-1}), but decreases toward the coast because of saline intrusion [*Knowles et al.*, 2007].

[9] The creek selected for this study is an ephemeral tributary to Pedler Creek that only flows during winter for several days or weeks after a large rain event. Winter 2011 was unusually dry, and only four single flow events were recorded between July and August (Figure 2). At the experimental site the creek channel is 1 m wide and approximately 0.5 m deep. The water table in the Quaternary aquifer is located 7 m below the streambed, so the stream is hydraulically disconnected from the groundwater at all times [*Brunner et al.*, 2011]. The soil profile comprises a gray dark silt loam approximately 0.5 m thick, overlying an unsaturated zone of yellowish silt clay loam with chalky nodules at different depths. The creek is incised into this profile, with the streambed comprising a thin layer of dark fine clay (approximately five centimeters thick). Streambed hydraulic conductivity measurements with a Guelph permeameter produced values ranging from 5.9×10^{-8} to 1.2×10^{-5} m s^{-1}, emphasizing the small-scale variability of hydraulic conductivity and the difficulty of using these values to calculate infiltration rates. Vegetation surrounding the stream is predominantly grass.

3. Methodology

3.1. Experimental Setup

[10] During summer 2011, when the creek was dry, a 7 m long section was isolated using metal sheets. These sheets, which were 2 m wide and 1.5 m high, were dug 40 cm into the streambed and bank, and sealed with bentonite (Figure 1). The 7 m stream length was chosen to be manageable and yet reduce edge effects, so that infiltration is predominantly two-dimensional. The streambed elevation between the metal sheets was surveyed using a Trimble R8 GNSS GPS receiver (±0.02 and ±0.03 m horizontal and vertical accuracy, respectively).

[11] The experiment was run for a total period of 5 days, from 21 to 26 March 2011. Water used in the experiment was stored in a 22 m^3 tank. From there, water was diverted to two smaller tanks (1.2 m^3 each), from which water was pumped into the stream. Use of the smaller tanks permitted more accurate monitoring of the pumping rate. To precisely monitor the pumping rate, a pressure transducer logger (In-Situ Inc. LevelTROLL 300 Series, ±0.2% accuracy), with a measuring interval of 5 min was installed in each of the smaller tanks, and manual measurements were periodically taken to verify the logger data. The water level of the creek was also continuously monitored using a pressure transducer logger and using a sight gauge. Effects of barometric fluctuations on water level readings were corrected using barometric data monitored every 5 min with an In-Situ Inc. BaroTROLL (±0.1% accuracy). Potential perched aquifers were expected to develop in the unsaturated zone due to clay layers extending beneath the site, so piezometers screened at different depths were equipped with pressure transducer loggers.

[12] Water was pumped into the creek to maintain a constant water level at three different increasing stages with time: 0.20, 0.31, and 0.38 m depth, for periods of 24, 48 and 48 h, respectively (Table 1). During each stage the water level was maintained by adjusting the pumping rate. During the period in which the water level is constant, the pumping rate is thus equal to the loss rate from the stream (infiltration plus evaporation). The volume of water leaking around the metal sheets was observed to be negligible. The change from one stage to another was achieved rapidly (within a period of 5 min) by increasing the pumping rate of water into the stream. The loss rate per unit length of

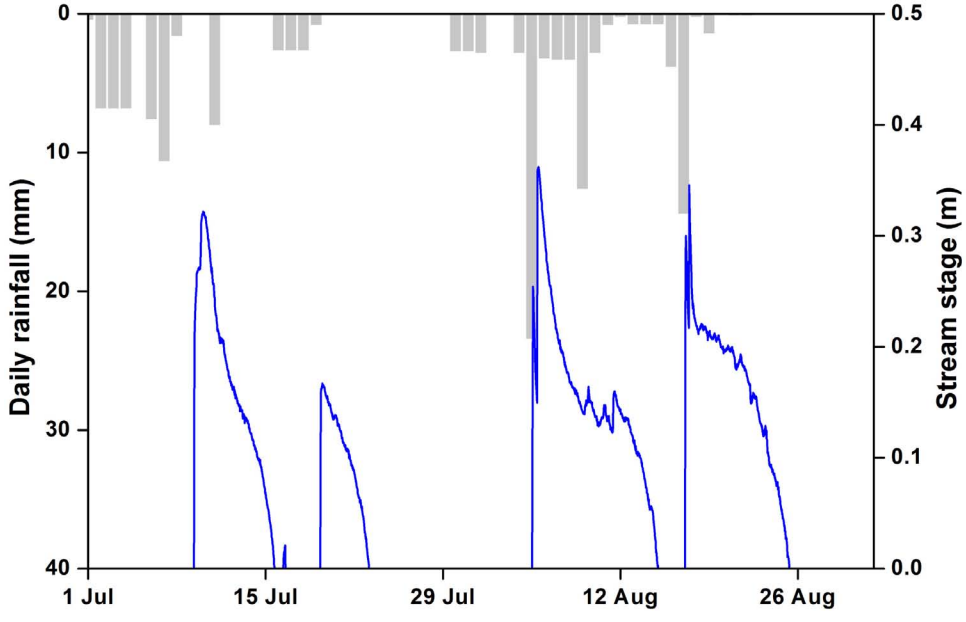

Figure 2. Stream stage under natural conditions at the experimental site (solid line) and daily rainfall recorded at Pirramina winery station, a 1.8 km distance to the experimental site (vertical bars).

Table 1. Characteristics of the Field Experimental Infiltration Test[a]

Stream Stage (m)	Duration (h)	Pumped Water (m^3)	Stream Storage Volume (m^3)	Infiltrated Volume (m^3)	Mean I_R ($m^3\ h^{-1}\ m^{-1}$)	Maximum Transient I_R ($m^3\ h^{-1}\ m^{-1}$)	I_R End of Stage ($m^3\ h^{-1}\ m^{-1}$)
1 (0–0.2)	24.0	5.10	0.57	4.53	0.027	0.076	0.012
2 (0.2–0.31)	48.0	6.90	1.26	6.21	0.018	0.049	0.015
3 (0.31–0.38)	48.0	7.50	2.04	6.72	0.020	0.039	0.018

[a] I_R = infiltration rate.

stream ($m^3\ h^{-1}\ m^{-1}$) was calculated at hourly intervals using changes in water level in the storage tanks, with an error of $\pm 1.3 \times 10^{-3}\ m^3\ h^{-1}\ m^{-1}$. When variations of the stream water level of more than 2 cm occurred, their effects on the infiltration rates were corrected by adding or subtracting the change in stream storage volume from the pumping rate.

[13] During the 5 days of experiment a total rainfall of 29 mm was recorded at the Pirramina Winery in McLaren Vale (Australian Government, Bureau of Meteorology Station num. 023876; 1.8 km distance from the study site), while the evaporation, estimated at Adelaide Airport (Australian Government, Bureau of Meteorology Station number 023034; 30 km distance to the study site) was 22.4 mm. These values give a net input of 0.04 m^3 of water to the stream transect (based on an open water surface of 7 m^2), which only represents 0.2% of the total pumped water into the creek during the experiment (19.5 m^3). Rainfall and evaporation were thus not considered in the calculation of stream water losses.

[14] Following the experiment the metal sheets were removed and water level within the stream monitored during natural flow events in July and August 2011 (Figure 2).

3.2. Modeling

[15] The goal of this work was to characterize infiltration from ephemeral streams as a function of stream level. As infiltration is measured directly, no effort was made to characterize the soil heterogeneity at the experimental site. The aim of the modeling is to allow extrapolation of infiltration rates to stream stages other than those reproduced in the field experiment. Model calibration, achieved by matching experimental infiltration rates, allowed us to determine bulk soil hydraulic parameters. Although the model fit could probably be improved by including soil heterogeneity in the model, this was not the aim of the project. Following model calibration, the same bulk parameters were then used to predict infiltration rates during natural flow events.

[16] A two-dimensional model orthogonal to the streamflow direction was developed using Hydrus 2-D [*Šimunek et al.*, 1998], which numerically solves the Richard's equation using a Galerkin-type linear finite element scheme. The modeled stream dimensions and topography reproduce the experimental site (Figure 3). The model comprises three layers. The soil zone, which extends from the surface to 0.5 m depth, is homogeneous but anisotropic, with the horizontal hydraulic conductivity component higher than its vertical. Below the soil zone, the unsaturated zone is modeled as homogeneous and isotropic. The third layer is a clogging layer, immediately underlying the streambed. It is modeled as homogeneous and isotropic, with a thickness of 5 cm thickness, thinning toward the edges of the streambed.

[17] Model discretization used 29,779 finite elements and 15,309 nodes, with mesh refinement beneath the streambed (1 cm spatial discretization, increasing with depth). No flow boundary conditions were applied at the vertical model edges, far enough from the area of interest to avoid boundary effects during modeling water infiltration. As the balance between rainfall and evaporation was negligible during the experiment, a no flow boundary condition was applied at the surface, except for the streambed, where a variable head boundary was set up to allow for changes in water depth. As vegetation surrounding the stream section is mainly grass and without woody plants, transpiration was not considered in modeling. The water table is represented, at the bottom of the vertical profile, by a constant pressure head boundary condition ($h = 0$).

[18] Initial conditions were obtained by linearly interpolating pressure head between the water table ($h = 0$) and the ground surface ($h = -100$ m). The pressure head of $h = -100$ m at the land surface is consistent with a dry soil (and streambed) during summer months. The model was first run under steady state conditions, with a dry streambed, using initial estimates of soil hydraulic parameters generated using the texture-based parameter values provided by Hydrus

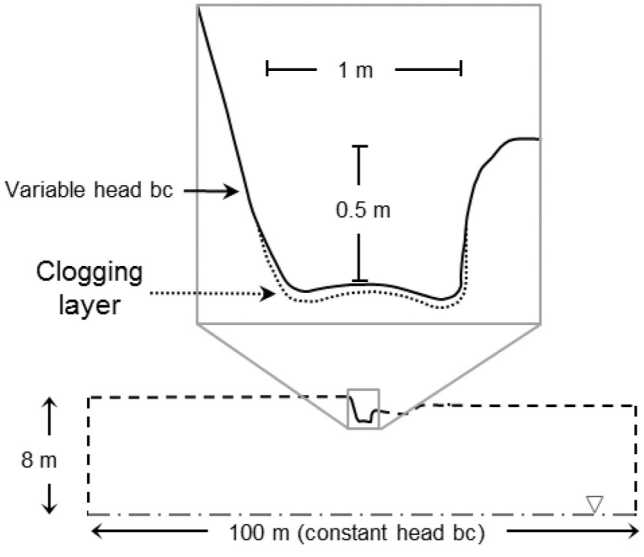

Figure 3. Geometry of the numerical model of the experimental stream, showing a detail of the streambed geometry and the permeable clogging layer underneath the streambed. A time variable head boundary condition was applied in the stream (solid line), and a constant head boundary condition was applied at the aquifer water table (dash-dotted line), while no-flow boundary conditions were applied elsewhere (dashed lines).

[*Carsel and Parrish*, 1988]. Results of the steady state simulation were subsequently used as the initial conditions for transient model calibration, where water levels in the creek were varied over time to reproduce water levels monitored during the experiment or under natural flow conditions.

[19] To estimate the hydraulic parameters of the subsurface materials, inverse modeling was accomplished using the Levenberg-Marquardt nonlinear weighted least squares approach [*Marquardt*, 1963] provided in Hydrus. The objective function was defined as the sum of the squared residuals between the field-measured and simulated infiltration rates over time. *Van Genuchten* [1980] expressions were used to parameterize the soil hydraulic properties:

$$S_e(\psi) = \frac{(\theta - \theta_r)}{(\theta_s - \theta_r)} = [1 + (\alpha|\psi|)^n]^{-m} \quad (1)$$

$$K(\psi) = K_s S_e^l [1 - (1 - S_e^{l/m})^m]^2 \quad (2)$$

where Ψ is matric potential or pressure head [L], K and K_s [L T^{-1}] are unsaturated and saturated hydraulic conductivities, respectively, S_e is the effective water saturation ($0 < S_e < 1$), θ_s, θ_r and θ are saturated, residual and actual volumetric water contents, respectively, α [L^{-1}] and n (dimensionless) are constants, where $m = 1 - 1/n$, and l is a pore connectivity parameter. The parameters optimized were θ_s, θ_r, α, n and K_s, while l was fixed at a value of 0.5 [*Mualem*, 1976].

[20] Because both evaporation and rainfall were negligible during the experiment, these processes were not included during the model calibration of the experiment. For subsequent model runs where infiltration and recharge processes following an ephemeral flow event were simulated, we considered evaporation from the wet streambed after cessation of flow. According to the estimated evaporation at the Adelaide Airport meteorological station during the experiment, a rate of 4.5 mm d^{-1} is used for this. Hydrus assumes that actual evaporation is equal to the potential evaporation until a critical surface pressure head is reached. After this point the evaporative flux at the soil surface decreases as the soil dries out and is no longer able to supply this water demand to the surface.

4. Results

4.1. Experimental Results

[21] A total of 19.5 m^3 were pumped into the stream over 5 days, comprising 5.1, 6.9 and 7.5 m^3 in stages 1 (24 h), 2 (48 h) and 3 (48 h), respectively (Figure 4a). A rapid increase of the water level at the beginning of the experiment and between stream stages was obtained, with relatively constant water levels maintained within each stage (Figure 4b). Although the lowest pumping volume corresponds to the first stream stage, it is worth noting that this volume was pumped in only 24 h, whereas stages 2 and 3 were maintained for 48 h. These volumes however do not correspond to the infiltrated volumes of water in each stream stage, as the change in storage between each stage must be first subtracted (Table 1).

[22] Infiltration rate with time per unit length of stream is highlighted in Figure 4c. These rates are only calculated after the water level of each stage had stabilized. Infiltration at each stage displayed an initial high rate which decreased over time, although none of the three stages clearly reached a steady state infiltration rate. The initial infiltration rate of stage 1 (0.076 m^3 h^{-1} m^{-1}) is higher than subsequent stages (0.049 and 0.039 m^3 h^{-1} m^{-1} for stage 2 and 3, respectively). Infiltration rate at the end of each stage was considerably lower, 0.013, 0.015 and 0.018 m^3 h^{-1} m^{-1}, respectively.

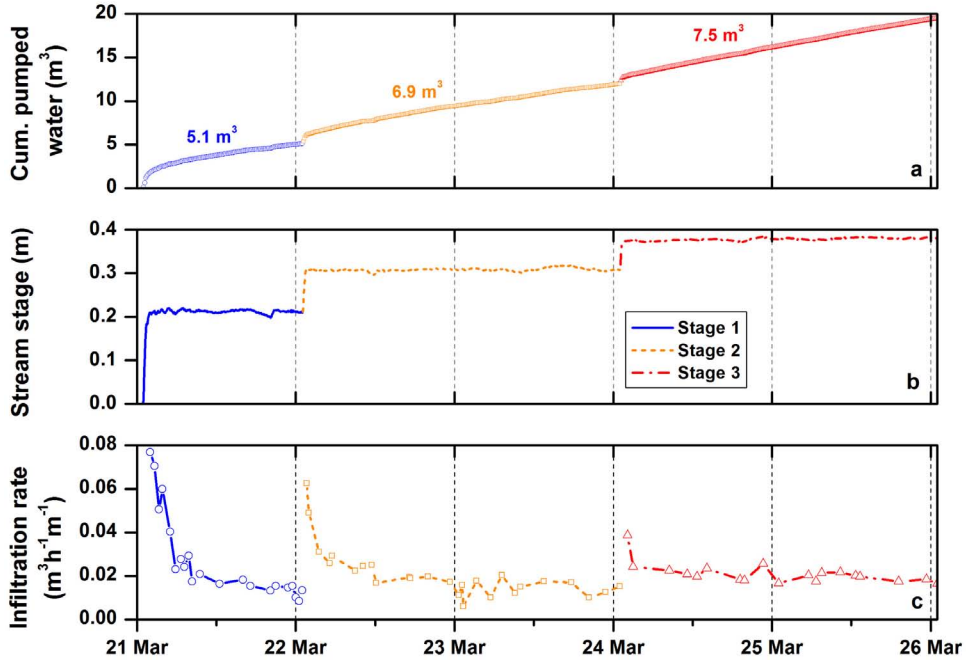

Figure 4. (a) Cumulative pumped water into the isolated stream reach, (b) stream stage measured in the creek during the infiltration experiment, and (c) field-measured experimental infiltration rates.

Mean infiltration rates, based on the total duration of each stage, were 0.027, 0.018 and 0.020 $m^3\ h^{-1}\ m^{-1}$ for stages 1, 2 and 3, respectively (Table 1). The contribution of the first hour to the total infiltrated volume strongly decreased as the stream water level rose, ranging from 19.3% in stage 1 to 4.4% in stage 3 (Table 2). The contribution of the first hour decreases for consecutive rising water levels because infiltration driven by capillary forces (i.e., sorptivity) decreases as the soil water content increases.

4.2. Modeling Results

4.2.1. Field Experiment

[23] A comparison of modeled and field-measured infiltration rates is presented in Figure 5, and optimized van Genuchten parameters for each of the three layers are shown in Table 3. The model reproduced all of the field measured infiltration rates, as well as the peak at each stage rise and transient dynamics. Optimized saturated hydraulic conductivities fall in the expected range for silt-clay loam sediments, and calibrated porosity values are in good agreement with soil moisture data monitored in the field, ranging between 0.37 and 0.45. Anisotropy within the top layer (low vertical hydraulic conductivity) was necessary to prevent capillary rise during the first stage of the experiment, and hence it allows us to simulate the magnitude of the transient response to subsequent stage rises.

[24] During 5 days of continuous infiltration none of the stages achieved steady infiltration rates, as evidenced by declining infiltration rates throughout each stage. Steady state simulations were also carried out (but are not shown here), where each stream stage was maintained until the infiltration rate stabilized. These simulations produced steady state infiltration rates of 0.010, 0.013 and 0.015 $m^3\ h^{-1}\ m^{-1}$ for stages 1, 2 and 3, respectively, approximately 1 order of magnitude lower than the initial transient rates measured during each stage of the experiment (Table 2). The water depth increased by 90% between stages 1 and 3 (0.2 to 0.38 m), while the steady state infiltration rate only increased by 50% (from 0.010 to 0.015 $m^3\ h^{-1}\ m^{-1}$).

[25] Modeled water content at the end of each stream stage is presented in Figure 6. During stage 1 the streambed wet perimeter is 1.3 m. Sediments adjacent to the wet area are fully saturated (Figure 6a). When the stream level rises from stage 1 to 2 (Figure 6b), and from 2 to 3 (Figure 6c), the streambed wet perimeter increases to 1.52 and 1.66 m, respectively, and the magnitude of the transient infiltration effect is related to this increase in the wet perimeter. However sediments between the stream wet perimeter 1 and 2 had already increased in water content during stream stage 1 due to capillary suction, and this reduces the magnitude of the transient effect (the same applies when the water level rises from stage 2 to stage 3). When stream level rises from stage 1 to stage 2, the increase in infiltration due to an increase of the wet perimeter was responsible of 31% of the transient infiltration, the rest being a consequence of changes in soil water content below the streambed.

[26] The cumulative infiltration at the completion of the five day experiment was 17.4 m^3. However, if we calculate the flux using steady state infiltration rate (0.010, 0.013 and 0.015 $m^3\ h^{-1}\ m^{-1}$ for stages 1, 2, and 3, respectively), we get 11.09 m^3 (Table 2). We would thus underestimate the total infiltrated volume by 36% (Table 2). However, over shorter time periods, the transient infiltration accounts for a much greater proportion of the infiltrated volume, so the shorter the flow duration, the greater the underestimation will be.

[27] The above discussion has focused on changes in infiltration rates as stream stage rises. Although rapid decreases in water level do not usually occur under natural conditions, we have simulated a rapid drop of the water level to illustrate and understand processes governing water infiltration under declining water levels. The calibrated model was therefore used to simulate infiltration in the case where stream level falls from one stage to another. Figure 7a shows changes in infiltration rate when the stream level decreases

Table 2. Field and Modeling Results of the Infiltration Experiment[a]

Transient Period (Field Values)						
	Stream Stage 1		Stream Stage 2		Stream Stage 3	
Time	V (m^3)	R (%)	V (m^3)	R (%)	V (m^3)	R (%)
1st h	0.87	19.30	0.39	6.30	0.30	4.38
12th h	3.39	75.61	2.22	35.70	2.01	29.75
24th h	4.53	100.00	3.72	59.90	3.66	52.34
48th h			6.21	100.00	6.72	100.00

Steady-State Period (Modeled Values)			
	Stream Stage 1	Stream Stage 2	Stream Stage 3
Infiltration Rate ($m^3\ h^{-1}\ m^{-1}$)	0.010	0.013	0.015

Total Experiment	Values
Cumulative pumped water (m^3)	19.50
Stream storage volume at stage 3 (m^3)	2.10
Mean infiltration rate ($m^3\ h^{-1}\ m^{-1}$)	0.021
Total Cumulative infiltration (m^3)	17.40
Total infiltrated volume if only steady infiltration rate considered (m^3)	11.09
Underestimated cumulative infiltration with only steady state rates (%)	36

[a]V = infiltrated volume; R = relative contribution of the stream stage to the total duration of the experiment.

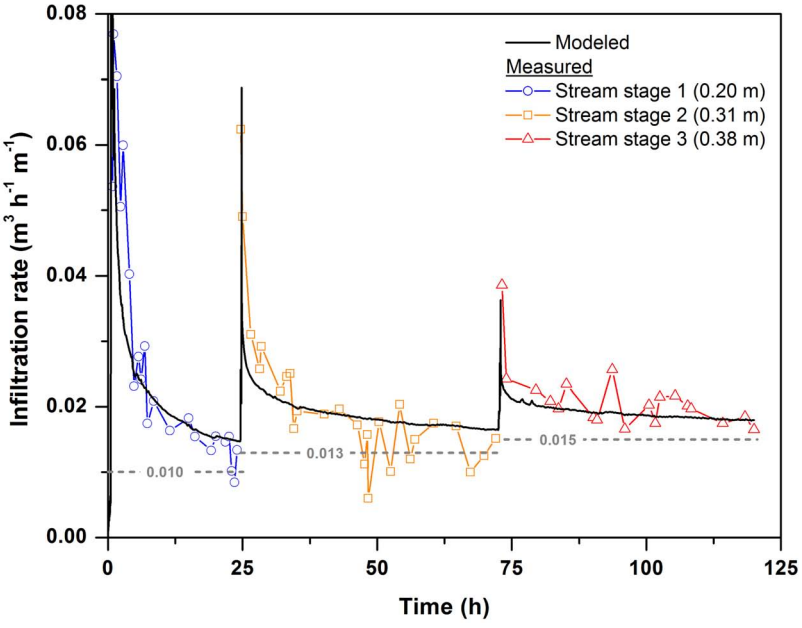

Figure 5. Experimental versus modeled infiltration rates. Dashed horizontal lines correspond to the modeled steady state infiltration rate of each stream stage.

from 0.38 m to 0.31 m. In this case, the simulation was run for a long period of time (365 days) before the stream stage was decreased, so that infiltration was initially at steady state. Following the decrease in stream stage, there is a rapid decrease in infiltration to below the steady state value corresponding to the new stream stage (0.31 m). The infiltration rate subsequently increases to the steady state value. The transient period of low infiltration is related to the time required for the soil water potentials to adjust to the new stream stage. Until the new equilibrium water potentials are reached, matric potentials beneath the streambed are higher than the equilibrium values, and hence the flux through the streambed is lower. Figure 7b shows changes in infiltration rate where the period of time at each stream stage is short. In this case, we have simply reversed the order of the stream stages from the experiment; i.e., 24 h at 0.38 m depth, followed by 48 h at 0.31 m and 48 h at 0.2 m. When the stream stage drops there is a sharp decrease in infiltration rate (i.e., at 24 and 72 h), but the infiltration rate then rises to above the steady state value. This is effectively a continuation of the high transient infiltration rate from the preceding stage. The reduction in infiltration rate immediately after the stream stage drop differs from Figure 7a because steady state infiltration rates were not achieved prior to reduction in stream stage.

Table 3. Calibrated van Genuchten Hydraulic Soil Parameters[a]

	Top Soil	Clogging Layer	Unsaturated Zone
θ_r	0.043	0.047	0.045
θ_s	0.42	0.36	0.38
α (m^{-1})	1.20	1.28	0.41
n	2.60	2.59	1.57
Kh_s ($m\ h^{-1}$)	2.85×10^{-2}	4.5×10^{-4}	2.7×10^{-3}
Kv_s ($m\ h^{-1}$)	4.75×10^{-3}	4.5×10^{-4}	2.7×10^{-3}
l[b]	0.5	0.5	0.50

[a] Kh_s and Kv_s are horizontal and vertical saturated hydraulic conductivity, respectively.
[b] Not calibrated, but fixed.

4.2.2. Natural Flow Event

[28] To quantify stream infiltration rates under natural flow conditions, the model was used to estimate infiltration during the first flow event in winter 2011 (Figure 2). River flow commenced on 9 July at 8:30 am, and the river stage increased rapidly to 0.2 m after only 1 h. A maximum stage of 0.32 m was reached after 17 h, after which the stream level gradually fell. The stream was dry 153 h after flow commenced (Figure 8a). Simulation of infiltration during this flow event produces a maximum infiltration rate of 0.023 m^3 h^{-1} m^{-1} after 1.8 h, decreasing to 0.015 m^3 h^{-1} m^{-1} half an hour later. It is noteworthy that the maximum infiltration rate is achieved while the stream level is still rising. A second peak in infiltration rate occurs as the stream level rises to 0.32 m, after which it steadily decreases (Figure 8b). The modeled total infiltration for this event was equal to 1.31 m^3 m^{-1}.

[29] The relationship between infiltration rates and stream level is shown in Figure 9. Most simulated infiltration rates are above the steady state line, particularly those at the beginning of the flow event: 3.9% of the total infiltration occurs during the first 2 h of the flow event, 31.5% occurs in the first 24 h, and the remaining 68.5% takes place in the remaining 128 h. The rate of change of steady state infiltration with change in water depth is more rapid above a stream level of 0.15 m. Below this point the wet perimeter is everywhere in contact with the clogging layer and consequently the infiltration rate is substantially reduced.

[30] The relationship between steady state infiltration rate and stream level can be used to determine the relative contributions of transient and steady state infiltration during the flow event. An infiltration of 0.88 m^3 m^{-1} would be

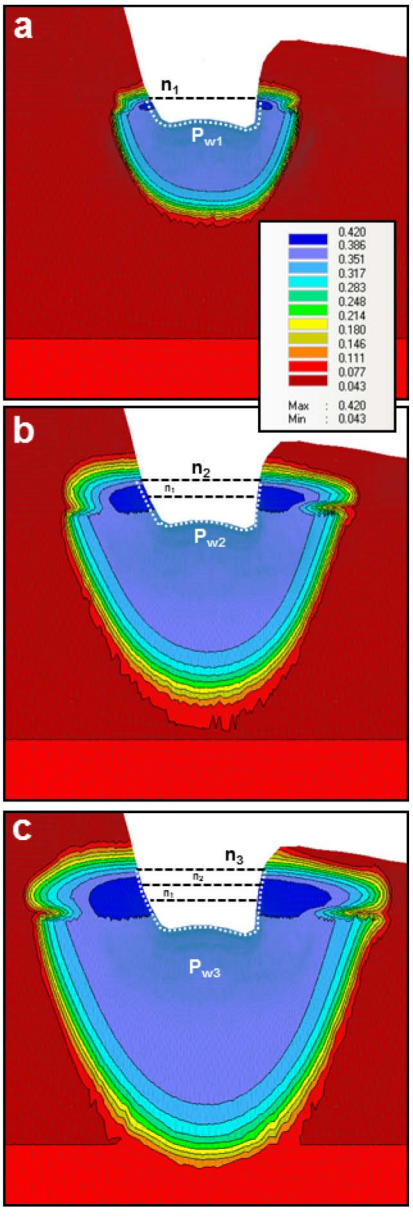

Figure 6. Modeled water content at the end of stream stages (a) 1 (n_1), (b) 2 (n_2), and (c) 3 (n_3). Dashed lines below the streambed show the wet perimeter (P_{wn}) of the corresponding *n* stream stage.

estimated using the steady state rates associated with each stream water level (shaded area below the dashed line in Figure 8b), whereas including transient infiltration gives a total infiltration of 1.31 m^3 m^{-1}. Neglecting transient infiltration would therefore result in underestimation of true infiltration by 33%, coincidentally a similar percentage to that obtained in the infiltration experiment (36%).

4.3. Infiltration Versus Recharge

[31] The contribution of infiltration to aquifer recharge was examined by simulating evaporation from the soil profile after completion of the flow event. Water that infiltrated during the flow event either drained to the water table (recharge) or was lost to evaporation (after ponding ceased and the streambed dried out). For these simulations, the potential evaporation rate was set to 4.5 mm d^{-1}. The simulation was then run until soil water content stabilized (a period of 270 days after flow ceased), resulting in no aquifer recharge, while the total infiltrated volume was 1.31 m^3 m^{-1}.

[32] The effect of flow duration was examined by modeling theoretical flow events of 0.25 m stream level of different duration, contrasting antecedent moisture content and different water table depths. In all cases, the stream level rose instantaneously to 0.25 m at the commencement of flow and fell to zero after flow ceased. The antecedent moisture content was established based upon linear pressure head distribution in the unsaturated zone, from $h = 0$ at the water table to $h = -15$ m at the land surface (wet conditions) or $h = -100$ m (dry conditions).

[33] For the deep water table and dry initial conditions (blue solid line in Figure 10a), a flow event lasting less than 15 days did not contribute to aquifer recharge. However, the same flow event, but with higher antecedent moisture content will start to recharge the aquifer after 10 days of flow (blue dashed line in Figure 10a). If the water table is 2 m below the streambed, infiltrated water reaches the aquifer more quickly in both, dry and wet soil conditions. A flow lasting for only 5 h will contribute to aquifer recharge if the soil is initially wet, while the flow will need to last for at least 12 h to contribute to aquifer recharge if the soil is initially dry. Figure 10b shows cumulative infiltration versus flow duration. The difference between wet and dry soil antecedent moisture content highlights the effect of the transient infiltration. Strong sorptivity forces at the beginning of the infiltration under dry soil conditions contribute to higher infiltration rates but not to higher recharge, as the water is primarily used to satisfy the water deficit of the unsaturated zone. This deficit is rapidly satisfied if the water table is close to the streambed surface.

5. Discussion

[34] The ponded infiltration experiment performed in this study has several advantages over traditional methods for characterizing infiltration from ephemeral streams. During our experiment, the streambed surface area that was sampled was approximately 7 m^2, between 2 and 4 orders of magnitude greater than is often sampled with traditional infiltrometer measurements or with lysimeters [*Callegary et al.*, 2007; *Lennartz et al.*, 2008; *Zou et al.*, 2001]. Furthermore, infiltrometers and lysimeters typically only sample the streambed, which can have different properties from stream banks [*Shope et al.*, 2012].

[35] *Dagès et al.* [2008] performed an infiltration experiment in a ditch section to study the role of these systems on groundwater recharge and contaminant dispersion on shallow aquifers. Their results highlighted the importance of these ephemeral systems to aquifer recharge, and the need to consider vertical and lateral flows to understand the wetting front propagation in the subsurface. However a single averaged infiltration rate was obtained, thereby neglecting differences between transient and steady state infiltration rates at changing stream stages. In our study we complement their results by studying the importance of transient

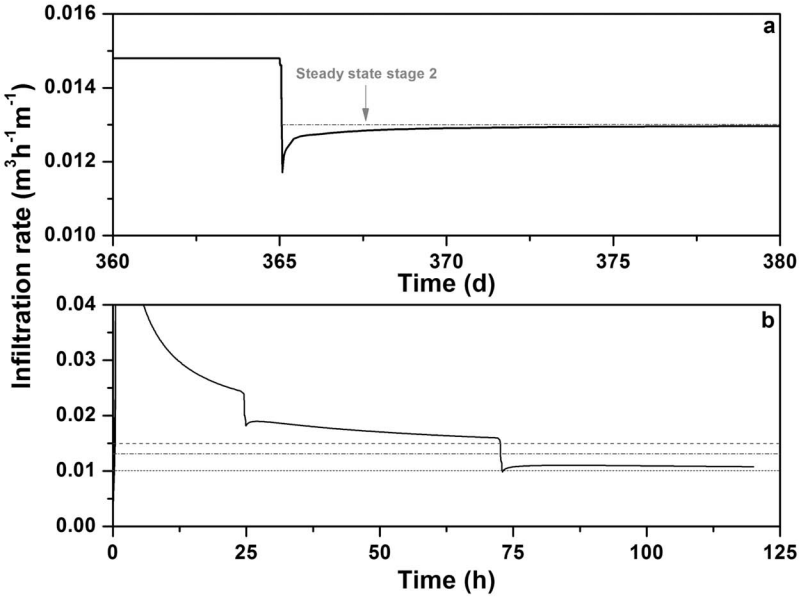

Figure 7. Modeled infiltration rates following a decrease in stream stage. (a) The model was initially run for 365 days with a stream depth of 0.38 m. Afterward, the stream stage was decreased to 0.31 m. (b) The model simulates a stream stage decrease from 0.38 to 0.31 after 24 h and from 0.31 to 0.20 m after 72 h, reproducing the reversed stream stages of the infiltration experiment. Steady state infiltration rates are 0.015, 0.013, and 0.010 $m^3\ h^{-1}\ m^{-1}$ at 0.38, 0.31, and 0.20 m and are indicated by long-dashed, dash-dotted, and short-dashed horizontal lines, respectively.

infiltration rate over steady state rates, not only at the onset of flow, but also at successive increasing stream stages.

[36] The infiltration experiment we performed is somehow similar to the recirculating furrow infiltrometer (RFI) method [*Blair and Trout*, 1989], a routine field infiltration experiment done to enhance agriculture irrigation efficiency. In this experiment, water is pumped into a furrow from a supply reservoir. At some distance down the furrow the water is collected and pumped back into the reservoir. Analogous to our experiment, the rate of change in water level in the supply reservoir is proportional to the infiltration rate of the soil in the test section, thus giving actual infiltration rates. More recently, the RFI was applied to study the effect of wet perimeters, flow section area, and initial soil water content

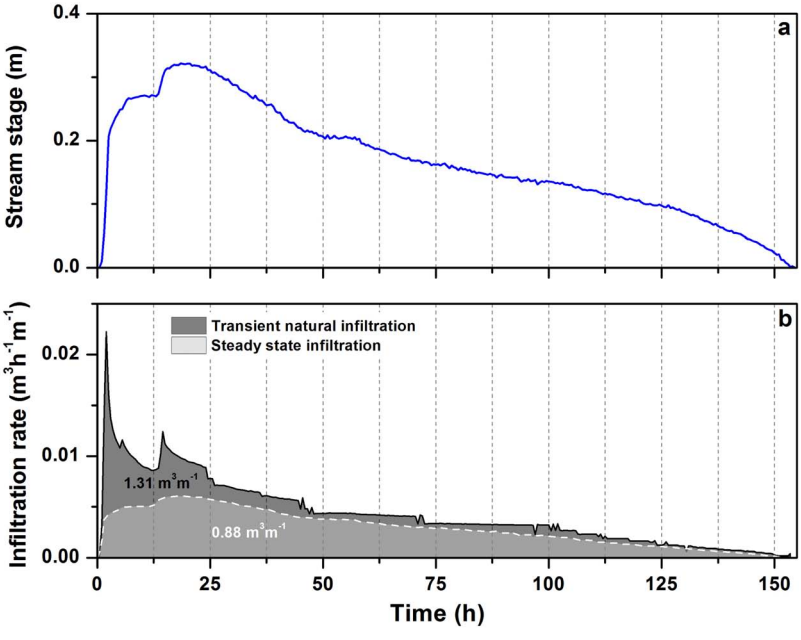

Figure 8. (a) Stream stage during the modeled natural flow event. (b) Modeled infiltration rates under transient natural conditions and only considering steady state infiltration rates (dashed line).

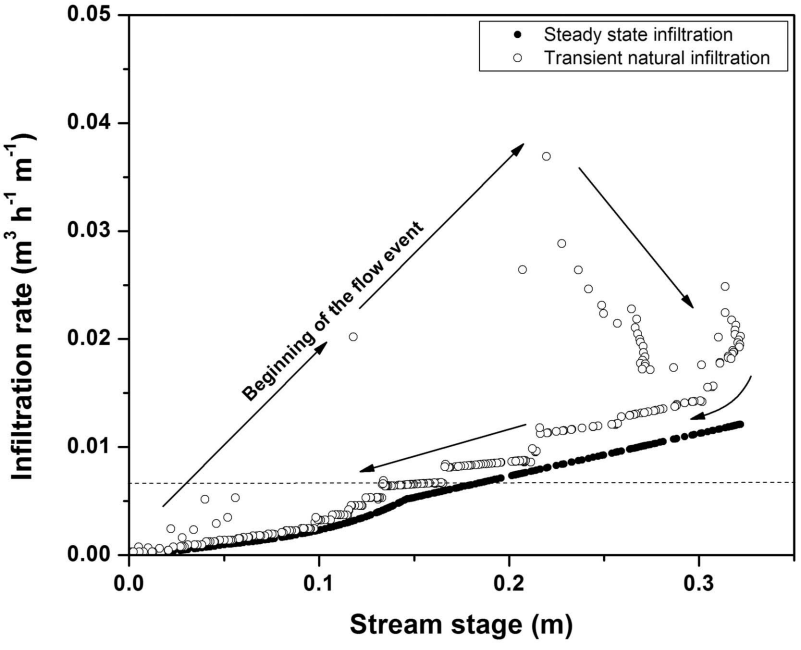

Figure 9. Modeled transient (circles) and steady state (dots) infiltration rates as a function of the stream stage. Arrows indicate progression of the natural infiltration event. Horizontal dashed line shows the approximate steady state infiltration rate (0.0065 $m^3\ h^{-1}\ m^{-1}$).

on furrow infiltration [*Zhang et al.*, 2012]. The decrease in flow rate with distance down the furrow reduces the sediment transport capacity causing deposition [*Trout*, 1999]. One of the advantages of the RFI method is that it can be used to investigate the effect of sediment transport on water infiltration. However, because the RFI requires pumping of water from the downstream to the upstream end of the furrow, it is not practical in large streams.

[37] The main limitation of our approach is that it does not simulate sediment scour and deposition processes, which have been shown to be significant, particularly in large high-energy streams [*Simpson and Meixner*, 2012; *Skolasińska*, 2006]. However, we do not believe that these processes are of major importance in Pedler Creek and its tributaries because of the low permeability of the streambed and the low energy of the flow events. One of the advantages

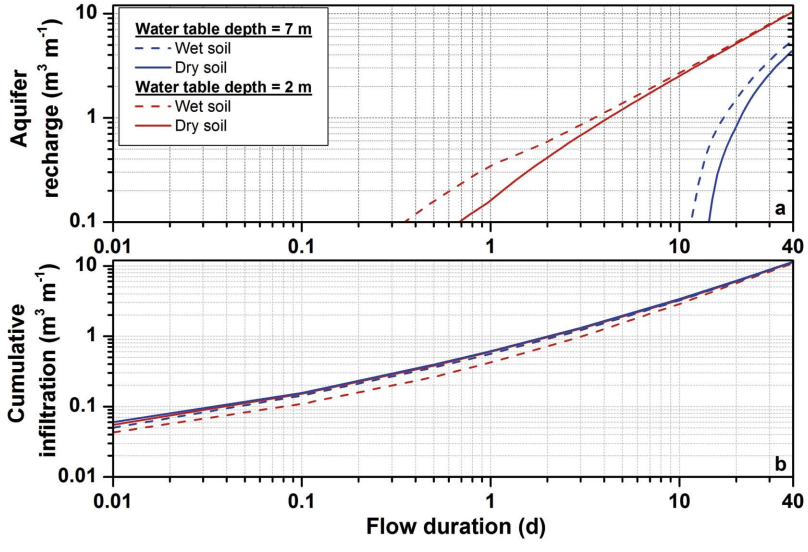

Figure 10. (a) Modeled flow duration needed to contribute to aquifer recharge, considering shallow (red lines) and deep (blue lines) water tables and dry (solid lines) and wet (dashed lines) antecedent soil moisture contents. Evaporation rate is 4.5 mm d^{-1} (only active after ponding water). Stream water depth during flow is 0.25 m. (b) Evolution of the cumulative infiltration water for different flow durations in shallow and deep aquifers under wet and dry antecedent moisture conditions.

of the approach we use is that it does not involve disturbance of the streambed.

[38] Our experiment allowed us to investigate changes in infiltration with increasing stream stage and during transient infiltration periods. There are currently little field data on these processes. Numerical simulations also provided information on changes in infiltration during falling stream stages, and on the relationship between infiltration and recharge.

5.1. Infiltration Versus Stream Stage

[39] Under steady state conditions, one-dimensional water infiltration in deep uniform soils (i.e., without clogging layer) will be by gravity drainage and hence equal to the saturated soil hydraulic conductivity, regardless of the depth of ponded water. However, if a clogging layer is present beneath the streambed, the infiltration flux at steady state will be [*Brunner et al.*, 2009]

$$q = K_c \frac{h_c + d - \gamma}{h_c} \tag{3}$$

where q [L T^{-1}] is the infiltration flux, d [L] is the depth of ponded water, h_c [L] is the thickness of the clogging layer, K_c [L T^{-1}] is the hydraulic conductivity of the clogging layer and γ [L] is the pressure head at the base of the clogging layer. If h_c is large the infiltration flux is independent of d, and approaches gravity drainage (with the flux equal to K_c). However if h_c and γ are small, the infiltration flux will be proportional to d. In our case, steady state infiltration rates increased by only 50% (from 0.010 to 0.015 m^3 h^{-1} m^{-1}) as the water depth increased by 90% (from 0.20 to 0.38 m). Although flow is clearly two dimensional, the proportional increase in flux is similar to that predicted by equation 3.

5.2. Relative Contribution of Transient and Steady State Infiltration

[40] Transient infiltration periods of less than an hour to several hours duration have previously been observed for ephemeral streams in similar climatic conditions in field [*Blasch et al.*, 2006] and modeling studies [*Freyberg*, 1983]. Our experimental results show that after two days steady state infiltration was not achieved, and modeled infiltration rates for a natural flow event show that more than 3 days were needed before infiltration rates approached steady state values. These results are in good agreement with those obtained by *Heilweil and Watt* [2011], who found that transient infiltration rates stabilized after 4 days of ponding trench infiltration, although the authors did not provide any explanation for this observation. Of course, the relative importance of transient infiltration to the total infiltration will decrease with flow duration. Our work has shown that high transient infiltration rates also occur following increases in stream level, and we do not believe that this phenomenon has been previously described.

[41] Streambed geometry plays a key role in stream infiltration. Greater wet area results in greater potential for infiltration [*Callegary et al.*, 2007]. Thus narrow channels with greater flow depths lead to less infiltration than wider channels with lower flow depths [*Mudd*, 2006]. However the bed morphology will not only affect the total volume of water infiltrated, but also the relative contribution of the transient infiltration period. The importance of transient infiltration as stream level rises is not only a function of how much the level rises, but also of the riverbed morphology. For rectangular shaped streams the increase in the stream level does not involve a significant increase of the bed surface area, thus the magnitude of the transient infiltration rate is expected to be lower. In our experimental site for example, the increase of wet perimeter was responsible of 31% of the transient infiltration. However, for V-shaped streams an increase of the stream level involves a considerable increase of the bed surface and thus wet perimeter, so the transient infiltration effect will be greater.

5.3. Water Infiltration and Aquifer Recharge

[42] At the onset of a flow event, the infiltrated water initially satisfies the soil moisture deficit of the unsaturated zone, and if infiltration persists, it will contribute to aquifer recharge once the storage capacity of the unsaturated zone is filled. For a flow event of finite duration, recharge will always be less than infiltration, because after the stream dries up, some of the infiltrated water will evaporate. If the flow duration is very short (and the water table is deep), most of the infiltrated water may evaporate and so recharge from the flow event will be low or zero. Importantly, while wet antecedent moisture content decreases the total infiltration during a flow event, it increases the total recharge from the same event. For conditions similar to those at our field site, it is estimated that flow events of 10–15 days are required to generate aquifer recharge. Transpiration rates of woody plants are usually much greater than evaporation rates [*Huxman et al.*, 2005; *Reynolds et al.*, 2000], and they are able to extract water from much greater depths. However, we only simulated evaporation from the streambed and not evapotranspiration from deep-rooted vegetation. Many arid zone rivers are lined with woody riparian vegetation, and in these cases, much longer flow durations will be required to produce significant recharge. For the same infiltrated volume, the importance of subsequent evaporation will also be greater in rivers with wide and flat streambeds than in narrow, deeper rivers.

6. Conclusions

[43] An infiltration experiment at the stream reach scale was performed to estimate infiltration rates during streamflow events. The experiment samples a much greater area than traditional methods, and provides information on infiltration through stream banks as well as through the streambed. The experiment and subsequent numerical modeling has shown that (1) transient infiltration rates, significantly above steady state infiltration rates, can persist for several days after flow commences; (2) transient infiltration rates will also occur when stream level increases; (3) the transient period significantly contributes to the total infiltrated volume; and (4) the antecedent soil moisture affects the transient infiltration rate and increases the total infiltrated volume under dry conditions, it does not increase the aquifer recharge.

[44] **Acknowledgments.** Funding for this research was provided by the National Centre for Groundwater Research and Training, an Australian government initiative, supported by the Australian Research Council and the National Water Commission. The authors gratefully thank Leconfield Vineyards for available access to the field site. Thanks are owed to Nicholas White, Lawrence Burk, Chani Welch, Louise Anders, Roger Cranswick,

Saskia Noorduijn, James McCallum, Mark Trigg, Margaret Shanafield, and Edward Banks for their availability and assistance during fieldwork. Special thanks go to Brenton Perkins for the design and construction of the metal dams, as well as his assistance in their field installation. Reviews of an early draft of the manuscript by Margaret Shanafield, Dirk Mallants, and Glenn Harrington are greatly appreciated. Subsequent reviews by three anonymous reviewers were also most beneficial.

References

Berndtsson, R., and M. Larson (1987), Spatial variability of infiltration in a semi-arid environment, *J. Hydrol.*, *90*(1–2), 117–133.

Blair, A. W., and T. J. Trout (1989), Recirculating furrow infiltrometer design guide, report, Cent. for Res. in Water Resour., Coll. of Eng., Univ. of Tex. at Austin, Austin.

Blasch, K. W., T. P. A. Ferré, J. P. Hoffmann, and J. B. Fleming (2006), Relative contributions of transient and steady state infiltration during ephemeral streamflow, *Water Resour. Res.*, *42*, W08405, doi:10.1029/2005WR004049.

Bruen, M. P., and Y. Z. Osman (2004), Sensitivity of stream-aquifer seepage to spatial variability of the saturated hydraulic conductivity of the aquifer, *J. Hydrol.*, *293*(1–4), 289–302.

Brunner, P., P. G. Cook, and C. T. Simmons (2009), Hydrogeologic controls on disconnection between surface water and groundwater, *Water Resour. Res.*, *45*, W01422, doi:10.1029/2008WR006953.

Brunner, P., P. G. Cook, and C. T. Simmons (2011), Disconnected surface water and groundwater: From theory to practice, *Ground Water*, *49*(4), 460–467.

Callegary, J. B., J. M. Leenhouts, N. V. Paretti, and C. A. Jones (2007), Rapid estimation of recharge potential in ephemeral-stream channels using electromagnetic methods, and measurements of channel and vegetation characteristics, *J. Hydrol.*, *344*(1–2), 17–31.

Calver, A. (2001), Riverbed permeabilities: Information from pooled data, *Ground Water*, *39*(4), 546–553.

Carsel, R. F., and R. S. Parrish (1988), Developing joint probability distributions of soil water retention characteristics, *Water Resour. Res.*, *24*(5), 755–769.

Childs, E. C., and M. Bybordi (1969), The vertical movement water in stratified porous material: 1. Infiltration, *Water Resour. Res.*, *5*(2), 446–459.

Constantz, J., A. E. Stewart, R. Niswonger, and L. Sarma (2002), Analysis of temperature profiles for investigating stream losses beneath ephemeral channels, *Water Resour. Res.*, *38*(12), 1316, doi:10.1029/2001WR001221.

Dagès, C., M. Voltz, J. G. Lacas, O. Huttel, S. Negro, and X. Louchart (2008), An experimental study of water table recharge by seepage losses from a ditch with intermittent flow, *Hydrol. Processes*, *22*(18), 3555–3563.

Dahan, O., B. Tatarsky, Y. Enzel, C. Kulls, M. Seely, and G. Benito (2008), Dynamics of flood water infiltration and ground water recharge in hyperarid desert, *Ground Water*, *46*(3), 450–461.

de Vries, J., and I. Simmers (2002), Groundwater recharge: An overview of processes and challenges, *Hydrogeol. J.*, *10*(1), 5–17.

Dunkerley, D. L. (2008), Bank permeability in an Australian ephemeral dry-land stream: Variation with stage resulting from mud deposition and sediment clogging, *Earth Surf. Processes Landforms*, *33*(2), 226–243.

Freyberg, D. L. (1983), Modelling the effects of a time-dependent wetted perimeter on infiltration from ephemeral channels, *Water Resour. Res.*, *19*(2), 559–566.

Fritz, B. G., D. P. Mendoza, and T. J. Gilmore (2009), Development of an electronic seepage chamber for extended use in a river, *Ground Water*, *47*(1), 136–140.

Guyonnet, D., N. Amraoui, and R. Kara (2000), Analysis of transient data from infiltrometer tests in fine-grained soils, *Ground Water*, *38*(3), 396–402.

Heilweil, V. M., and D. E. Watt (2011), Trench infiltration for managed aquifer recharge to permeable bedrock, *Hydrol. Processes*, *25*(1), 141–151.

Horton, R. E. (1940), An approach towards a physical interpretation of infiltration capacity, *Proc. Soil Sci. Soc. Am.*, *5*, 399–417.

Huxman, T. E., B. P. Wilcox, D. D. Breshears, R. L. Scott, K. A. Snyder, E. E. Small, K. Hultine, W. T. Pockman, and R. B. Jackson (2005), Ecohydrological implications of woody plant encroachment, *Ecology*, *86*(2), 308–319.

Kalbus, E., C. Schmidt, J. W. Molson, F. Reinstorf, and M. Schirmer (2009), Influence of aquifer and streambed heterogeneity on the distribution of groundwater discharge, *Hydrol. Earth Syst. Sci.*, *13*(1), 69–77.

Knowles, I., M. Teubner, A. Yan, P. Rasser, and J. Lee (2007), Inverse groundwater modelling in the Willunga Basin, South Australia, *Hydrogeol. J.*, *15*(6), 1107–1118.

Lee, D. R. (1977), A device for measuring seepage flux in lakes and estuaries, *Limnol. Oceanogr.*, *22*(1), 140–147.

Lennartz, B., N. Jarvis, and F. Stagnitti (2008), Effects of heterogeneous flow on discharge generation and solute transport, *Soil Sci.*, *173*(5), 306–320.

Marquardt, D. W. (1963), An algorithm for least-squares estimation of nonlinear parameters, *SIAM J. Appl. Math.*, *11*, 431–441.

Mein, R. G., and C. L. Larson (1973), Modeling infiltration during a steady rain, *Water Resour. Res.*, *9*(2), 384–394.

Mualem, Y. (1976), A new model for predicting the hydraulic conductivity of the unsaturated porous media, *Water Resour. Res.*, *12*(3), 513–522.

Mudd, S. M. (2006), Investigation of the hydrodynamics of flash floods in ephemeral channels: Scaling analysis and simulation using a shock-capturing flow model incorporating the effects of transmission losses, *J. Hydrol.*, *324*(1–4), 65–79.

Murdoch, L. C., and S. E. Kelly (2003), Factors affecting the performance of conventional seepage meters, *Water Resour. Res.*, *39*(6), 1163, doi:10.1029/2002WR001347.

Perroux, K. M., and I. White (1988), Designs for disc permeameters, *Soil Sci. Soc. Am. J.*, *52*(5), 1205–1215.

Reynolds, J. F., P. R. Kemp, and J. D. Tenhunen (2000), Effects of long-term rainfall variability on evapotranspiration and soil water distribution in the Chihuahuan Desert: A modeling analysis, *Plant Ecol.*, *150*(1), 145–159.

Ronan, A. D., D. E. Prudic, C. E. Thodal, and J. Constantz (1998), Field study and simulation of diurnal temperature effects on infiltration and variably saturated flow beneath an ephemeral stream, *Water Resour. Res.*, *34*(9), 2137–2153.

Rosenberry, D. O., and J. Pitlick (2009), Local-scale variability of seepage and hydraulic conductivity in a shallow gravel-bed river, *Hydrol. Processes*, *23*(23), 3306–3318.

Rosenberry, D. O., P. Z. Klos, and A. Neal (2012), In situ quantification of spatial and temporal variability of hyporheic exchange in static and mobile gravel-bed rivers, *Hydrol. Processes*, *26*(4), 604–612.

Shope, C. L., J. E. Constantz, C. A. Cooper, D. M. Reeves, G. Pohll, and W. A. McKay (2012), Influence of a large fluvial island, streambed, and stream bank on surface water-groundwater fluxes and water table dynamics, *Water Resour. Res.*, *48*, W06512, doi:10.1029/2011WR011564.

Simpson, S. C., and T. Meixner (2012), Modeling effects of floods on streambed hydraulic conductivity and groundwater-surface water interactions, *Water Resour. Res.*, *48*, W02515, doi:10.1029/2011WR011022.

Šimunek, J., K. Huang, and M. T. van Genuchten (1998), The HYDRUS code for simulating the one-dimensional movement of water, heat and multiple solutes in variably-saturated media, version 6, *Res. Rep. 144*, 164 pp., U.S. Salinity Lab., Agric. Res. Serv., U.S. Dep. of Agric., Riverside, California.

Skolasińska, K. (2006), Clogging microstructures in the vadose zone—Laboratory and field studies, *Hydrogeol. J.*, *14*(6), 1005–1017.

Sophocleous, M. A. (1991), Combining the soilwater balance and water-level fluctuation methods to estimate natural groundwater recharge: Practical aspects, *J. Hydrol.*, *124*, 229–241.

Sorman, A. U., M. J. Abdulrazzak, and H. J. Morel-Seytoux (1997), Groundwater recharge estimation from ephemeral streams. Case study: Wadi Tabalah, Saudi Arabia, *Hydrol. Processes*, *11*(12), 1607–1619.

Trout, T. J. (1999), Sediment transport in irrigation furrows, in *Sustaining the Global Farm: Selected Papers From the 10th International Soil Conservation Organization Meeting*, edited by D. E. Stott, R. H. Mohtar, and G. C. Steinhardt, pp. 710–716, Purdue Univ., West Lafayette, Indiana.

van Genuchten, M. T. (1980), A closed-form equation for predicting the hydraulic conductivity of unsaturated soils, *Soil Sci. Soc. Am. J.*, *44*(5), 892–898.

Zhang, Y., P. Wu, X. Zhao, and P. Li (2012), Evaluation and modelling of furrow infiltration for uncropped ridge–furrow tillage in Loess Plateau soils, *Soil Res.*, *50*(5), 360–370.

Zou, Z. Y., M. H. Young, Z. Li, and P. J. Wierenga (2001), Estimation of depth averaged unsaturated soil hydraulic properties from infiltration experiments, *J. Hydrol.*, *242*(1–2), 26–42.